(8) Schaefer, J.; McKay, R. A.; Stejskal, E. O. *J. Magn. Reson.* **1979**, *34*, 443.
(9) Schaefer, J.; Stejskal, E. O.; Garbow, J. R.; McKay, R. A. *J. Magn. Reson.* **1984**, *59*, 150.
(10) McKay, R. A.; Schaefer, J.; Stejskal, E. O.; Ludicky, R.; Matthews, C. N. *Macromolecules* **1984**, *17*, 1124.
(11) Schaefer, J.; McKay, R. A.; Stejskal, E. O.; Dixon, W. T. *J. Magn. Reson.* **1983**, *52*, 123.
(12) Dixon, W. T. *J. Chem. Phys.* **1982**, *77*, 1800.
(13) Schaefer, J.; Stejskal, E. O. *Top. Carbon-13 NMR Spectrosc.* **1979**, *3*, 384.
(14) Hester, R. K.; Ackerman, J. L.; Neff, B. L.; Waugh, J. S. *Phys. Rev. Lett.* **1976**, *36*, 1081.
(15) Stoll, M. E.; Vega, A. J.; Vaughn, R. W. *J. Chem. Phys.* **1976**, *65*, 4093.
(16) Waugh, J. S.; Huber, L. M.; Haeberlen, U. *Phys. Rev. Lett.* **1968**, *20*, 180.
(17) Munowitz, M. G.; Griffin, R. G.; Bodenhausen, G.; Huang, T. H. *J. Am. Chem. Soc.* **1981**, *103*, 2529.
(18) Munowitz, M. G.; Griffin, R. G. *J. Chem. Phys.* **1982**, *76*, 2848.
(19) Schaefer, J.; Stejskal, E. O.; McKay, R. A.; Dixon, W. T. *Macromolecules* **1984**, *17*, 1479.
(20) Schaefer, J.; Stejskal, E. O.; Perchak, D.; Skolnick, J.; Yaris, R. *Macromolecules* **1985**, *18*, 368.
(21) Mansfield, P.; Orchard, M. J.; Stalker, D. C.; Richards, K. H. B. *Phys. Rev.* **1973**, *37*, 90.
(22) Rhim, W. K.; Elleman, D. D.; Vaughn, R. W. *J. Chem. Phys.* **1973**, *59*, 3740.
(23) Burum, D. P.; Linder, M.; Ernst, R. R. *J. Magn. Reson.* **1982**, *44*, 173.
(24) Herzfeld, J.; Berger, A. E. *J. Chem. Phys.* **1980**, *73*, 6021.
(25) Verbist, J. J.; Lehmann, M. S.; Koetzle, T. F.; Hamilton, W. C. *Acta Crystallogr., Sect. B* **1972**, *B28*, 3006.
(26) Greenfield, M. S.; Vold, R. L.; Vold, R. R. *J. Chem. Phys.* **1985**, *83*, 1440.
(27) Fuks, R. *Tetrahedron* **1973**, *29*, 2147.
(28) See, for example: Witanowski, M.; Stefaniak, L.; Webb, G. A. In *Annual Reports in NMR Spectroscopy*; Webb, G. A., Ed.; Academic: New York, 1981; Vol. IIB.
(29) Ebdon, J. R.; Heaton, P. E.; Huckerby, T. N.; O'Rourke, W. T. S.; Parkin, J. *Polymer* **1984**, *25*, 821.
(30) Cain, A. H.; Sullivan, G. R.; Roberts, J. D. *J. Am. Chem. Soc.* **1977**, *99*, 6423.
(31) Völker, T. *Angew. Chem.* **1960**, *72*, 379.

# Structure of Iodide Ions in Iodinated Nylon 6 and the Evolution of Hydrogen Bonds between Parallel Chains in Nylon 6

**N. S. Murthy**

*Corporate Technology, Allied-Signal Inc., Morristown, New Jersey 07960.*
*Received April 2, 1986*

ABSTRACT: Iodine is present as $I_5^-$ and $I_3^-$ ions in iodine–nylon 6 complexes obtained by immersing nylon 6 in an aqueous solution of $KI/I_2$. Low-angle X-ray scattering data indicate that in fresh samples the concentration of potassium or iodide ions, or both, is higher in the crystalline lamellar regions than in the interlamellar amorphous regions. It is possible that in some instances iodide ions form sheets and are intercalated between sheets of nylon 6 chains to form a paracrystalline lattice. Two types of $I_5^-$ columns are identified: in the less stable form the average iodine–iodine distance is 3.2 Å; in the more stable form this distance is 3.08 Å. The $I_5^-$ ions columns (probably $H^+I_5^-$) interact strongly with nylon 6 molecules and are oriented along the chain axis. The $I_3^-$ ions (probably $K^+I_3^-$) are weakly bound to nylon 6 and are oriented normal to the chain axis. These intrinsic relations between the iodide ion columns and the nylon chains and the unidirectional diffusion of iodide ions from the surface to the interior of a film causes oriented crystallization of unoriented mobile amorphous regions. This results in the preferential orientation of the crystalline regions in unoriented precursor films immediately after iodination, so that the polymer chains are normal to the surface of the film. Wide-angle X-ray diffraction results suggest that the commensurate structure of $I_5^-$ columns (average iodine–iodine distance of 3.2 Å) with the nylon 6 chains results in a 15.8–16.0 Å repeat in nylon 6, the shortest observed thus far, which twists the H-bonds out of the plane of the H-bonded sheet. During desorption of the iodine, H-bonds are now readily formed between parallel chains, the chain repeat increases to 16.7–16.9 Å, and the amide groups in the adjacent H-bonded sheets align in one plane. This is usually designated the $\gamma$ form of nylon 6.

## Introduction

Iodine complexes of polymers are important for many reasons. For example, poly(vinylpyridine)–iodine complexes[1] and nylon 6–iodine complexes[2] can be used as electrode materials in lithium–iodide batteries. Some iodine complexes such as polyacetylene–iodine are also good electrical conductors.[3] When KI is used as a heat stabilizer in engineered parts made from nylon 6, it is quite possible that the iodide ions play an active role. Iodine has two additional effects in nylon 6: it transforms the amorphous or the $\alpha$ form of nylon 6 into the $\gamma$ form[4] (in the $\alpha$ form[5] the hydrogen bonds are formed between fully extended antiparallel chains producing a chain repeat of 17.2 Å; in the $\gamma$ form[4] these hydrogen bonds are between parallel chains, resulting in a shorter chain repeat of 16.9 Å), and the diffusion of iodine into unoriented films causes the polymer chains to orient normal to the surface of the film.[6,7] To understand the effects of iodine in polymers in general, we studied the most readily available complex, i.e., iodine–nylon 6. Here we report on the structure of iodide ions and nylon 6 molecules in the complex. We discuss the diffusion-induced oriented crystallization and the resulting orientation of the polymer chains. Finally, we follow the changes in the iodide ion arrays and the changes in the conformation of the nylon 6 chains during iodine desorption.

## Materials and Methods

Commercially available nylon films made by Allied Corp. were used in most of our experiments (intrinsic viscosity 1.34 dL/g; $M_n \approx 19000$; $M_w \approx 38000$; sodium stearate <0.1%; oligomers (up to $n = 6$) including caprolactam <1%; crystallinity of the rolled film ~15% (mixture of $\alpha$ and $\gamma$); crystallinity of the drawn (1:3) film ~50% (mostly $\alpha$); crystallite size in the drawn film ~45 Å). Uniaxial orientation was obtained by stretching these films by 1:3 at room temperature. The films were iodinated by immersing the films in an aqueous solution of 1.23 M potassium iodide and 1.23 M iodine for periods ranging from 5 min to 16 h. The term freshly prepared sample is used to designate these iodinated films

0024-9297/87/2220-0309$01.50/0 

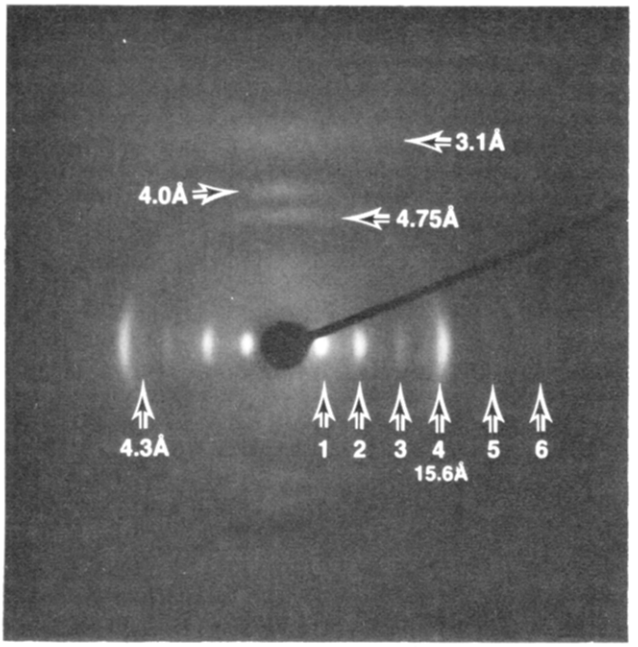


**Figure 1.** X-ray diffraction photograph of an oriented (drawn 1:3) complex. Up to 8 orders of the 15.6-Å repeat can be seen on the equator along with a shoulder at 4.3 Å corresponding to the (200) reflection of nylon 6. Of the three intense reflections on the meridian, the middle reflection at ~4.0 Å is due to the fiber axis repeat of nylon 6, and the diffuse bands at 4.75 and 3.1 Å are due to iodide ion columns.

after rinsing with water to remove excess $KI/I_2$ from the surface of the film and drying between filter papers for ~30 min. Iodine was desorbed by immersing either in water or in 0.1 M aqueous solution of thiosulfate for various lengths of time. Films taken out for analysis during washing in aqueous sodium thiosulfate but before complete extraction of $KI/I_2$ will be referred to as partially desorbed specimens. Iodinated samples that were left exposed to ambient atmosphere, and in which no deliberate attempt was made to extract $KI/I_2$, will be labeled as aged specimens.

X-ray diffraction (XRD) results were obtained under ambient condition by using copper radiation. XRD photographs were taken on a Unicam camera with a Ni filter and a sample-to-film distance of 4 cm. XRD scans were obtained on a Philips diffractometer with a graphite monochromator in the diffracted beam. Parafocus or transmission scans were obtained depending on the desired data. During the final stages of the project, transmission X-ray diffraction patterns were obtained by using a two-dimensional position-sensitive detector (Xentronics) mounted on a Huber goniometer. Small-angle X-ray scattering data were obtained on a linear position-sensitive detector mounted on a Franks camera.[8]

We noticed that the diffraction peaks from iodide ion columns were not symmetrical about the maximum, but rose sharply on the low-angle side of the maximum and tailed off gradually toward higher angles. Bragg spacings of such peaks were calculated by using appropriate correction factors.[9]

## Results

An XRD photograph of a nylon 6–iodine complex of an oriented film is shown in Figure 1 for the purpose of indicating the meridional and equatorial reflections. Figure 2 shows equatorial scans obtained in the parafocus geometry from iodinated planar oriented films in which the hydrogen-bonded sheets in nylon 6 are parallel to the plane of the film. One can see up to 12 orders of a 15.6-Å repeat along the equator (Figure 2A), together with a weak reflection at 4.3–4.4 Å just inside the fourth order of the 15.6-Å spacing (Figure 1). Meridional reflections at 4.75 and 4 Å and a diffuse band at ~3.1 Å can also be seen in the photograph. We attribute the 15.6-Å series to the

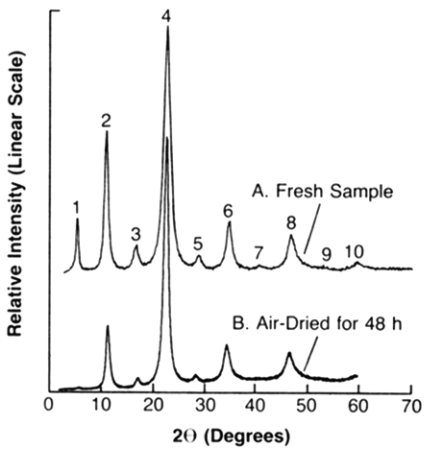


**Figure 2.** X-ray diffractometer scan (parafocus geometry) of planar-oriented iodinated nylon 6 film. Curve A is from a film during early stages of iodine desorption. Curve B is from a film during later stages of iodine desorption. The 10 orders of the 15.6-Å repeat are identified in curve A.

intercalation of two-dimensional iodide ion sheets between sheets of nylon 6 chains (possibly hydrogen-bonded sheets), the 4.3-Å reflection to the hydrogen-bonded nylon 6 chains, the 4.75-Å meridional reflection to the separation of $I_3^-$ arrays, the 4-Å reflection to the meridional (040) reflection of the fiber axis repeat (15.8–16.0 Å) of nylon 6, and the meridional band at 3.1 Å to the iodine–iodine distances in $I_5^-$ columns.

Typical data used in identifying the various reflections are shown in Figures 3 and 4. These are a series of parafocus and transmission scans at various stages of iodine desorption from initially unoriented films. One new observation from these results is the occurrence of two average iodine–iodine distances in the iodide ion columns in our complexes. The 3.1-Å asymmetric peak, which was earlier assigned to just one iodine–iodine distance,[7] is actually composed of two asymmetric peaks with $d$ spacings of 3.2 and 3.08 Å (Figure 5). The 3.2-Å peak is present only in freshly prepared samples. As the iodine is desorbed, either by washing in a dilute aqueous solution of sodium thiosulfate for a few minutes or by aging under ambient conditions for a day, the intensity of the 3.2-Å reflection decreases along with the intensity of the lower angle 4.75-Å iodine-column asymmetric peak. The 3.08-Å peak is present till the final stages of iodine desorption. Other observations from several such studies, as well as from analyses of oriented complexes, are given below.

1. The intensity of the meridional 3.2- and 4.75-Å asymmetric reflections decreases at about the same rate during the initial stages of desorption (Figure 5). A shoulder begins to appear at 8 Å ($2\theta \approx 11°$ along the meridian) as these two bands disappear.

2. The 15.6-Å equatorial series disappears almost simultaneously with the 4.75-Å meridional asymmetric reflection (Figures 3B and 4B).

3. In many instances, the intensities of the odd orders of 15.6 Å decrease faster than those of the even orders (Figure 2B), and in some aged specimens only even orders are present. Figure 6 shows an example where only even orders of 15.6 Å series are present. In such specimens, the 8- and the 4-Å reflections of nylon 6 and the 3.1-Å band from the iodide ion columns are present on the meridian (Figures 3B and 4B). The chain-axis repeat of nylon 6 in the complex, as estimated from the 8- and 4-Å meridional reflections, varies from 15.8 to 16.0 Å.

4. At later stages of iodine desorption the repeat of the 4-Å nylon 6 reflection on the meridian increases to 4.1 Å,

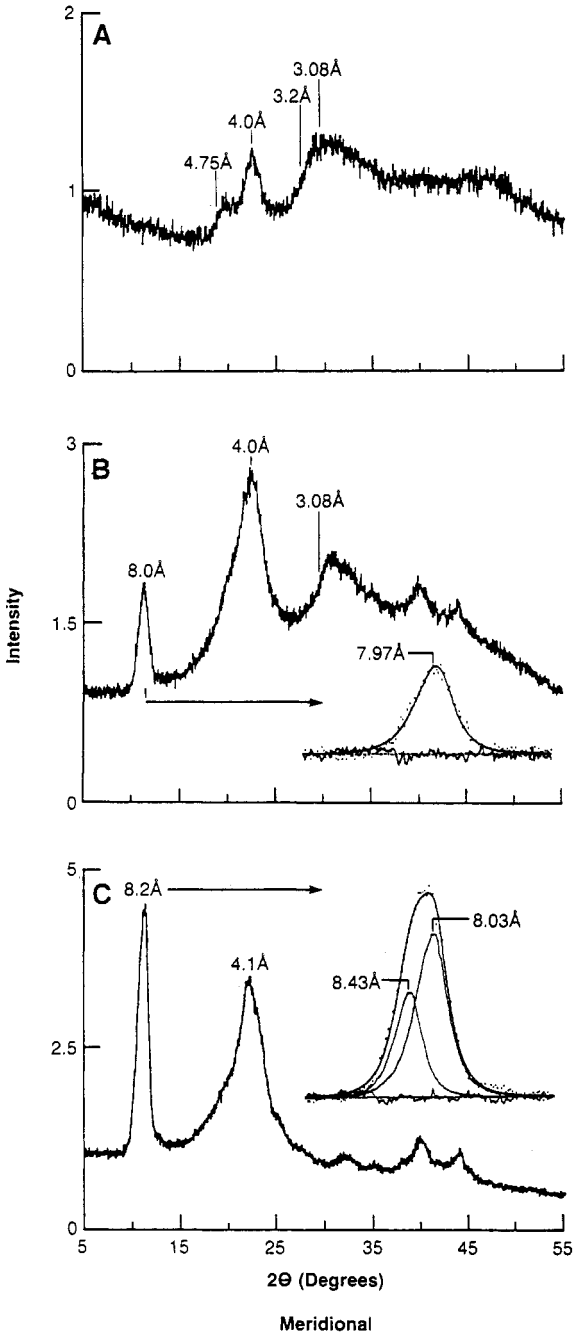


**Figure 3.** X-ray diffractometer scan (parafocus mode) of initially unoriented iodinated nylon 6 film at various stages of iodine desorption. The *d* spacings of the peaks are shown in the figure. The insets in parts B and C show detailed profile analysis of the 8-Å reflection. Data points, fitted curve (full line), resolved components (full line in C), base line (points), and the residue (difference between the obesrved and fitted intensity values, full line about the base-line points) are shown in these insets.

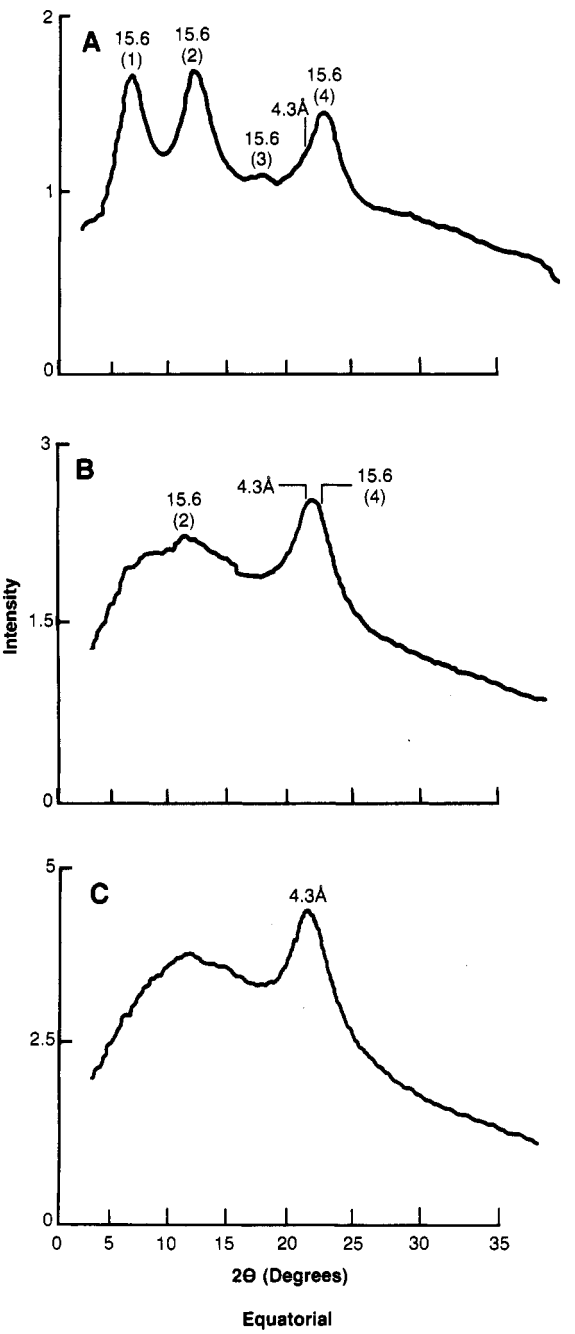


**Figure 4.** Transmission scans of the films used in Figure 3. Four orders of the 15.6-Å repeat and the 4.3-Å peaks are shown in the figure.

and this increase is accompanied by an increase in the intensity of the (020) reflection of nylon 6 at 8 Å ($2\theta = 11°$ along the meridian; Figures 3C and 4C). We attribute this 8-Å peak to nylon 6, since this peak does not appear in freshly prepared samples (Figures 1 and 3A). As can be seen from the resolved profiles in parts B and C of Figure 3, the increase in the intensity of the 8-Å reflection is accompanied by a shift in the position of the peak from 7.95 to 8.43 Å (chain-axis repeat increases from 15.9 to 16.9 Å).

5. During the final stages of iodine desorption, the meridional 3.08-Å band disappears, and the fiber repeat, calculated from (020) and (040) reflections, increases to 16.7–16.9 Å (Figure 7D, photograph).

6. The iodide ion column reflections (the 4.75-, 3.2-, and 3.08-Å peaks) are asymmetric with a steep rise in intensity of the low-angle side of the maximum and a slower decrease toward higher angles. This feature is obvious in Figure 3A and in the upper curve in Figure 5 for the 4.75-Å peak and in Figure 3B and in the lower curve in Figure 5 for the 3.08-Å peak. Evidence for the asymmetry of the 3.2-Å peak is indirect since it requires the assumption that a scan from a fresh sample (Figure 3A) has only a small contribution from the 3.08-Å peak. This assumption is reasonable since the intensity from the 3.2-Å iodide–iodine repeat decreases during aging (Figure 5) while the 3.08-Å iodide-iodine repeat is dominant in partially desorbed (Figure 3B) or aged (lower curve in Figure 5) specimens. Since the asymmetry of the 4.75-Å peak was not observed in our earlier work,[7] the necessary correction factors[9] were

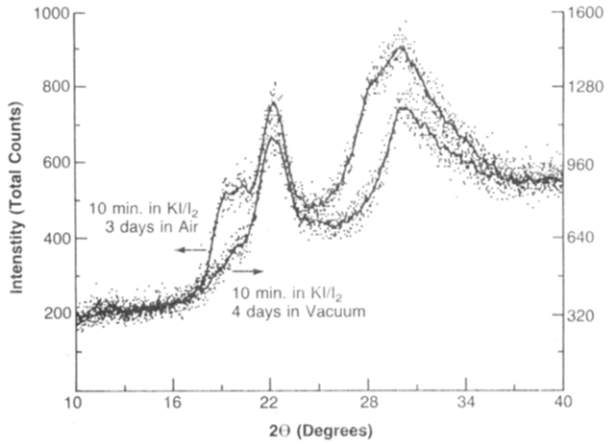


**Figure 5.** Comparison of 4.75-, 3.2-, and 3.08-Å iodine column reflections at two stages of iodine desorption. Data (1 s per 0.02° $2\theta$ step) were collected in parafocus geometry from unoriented precursor films.

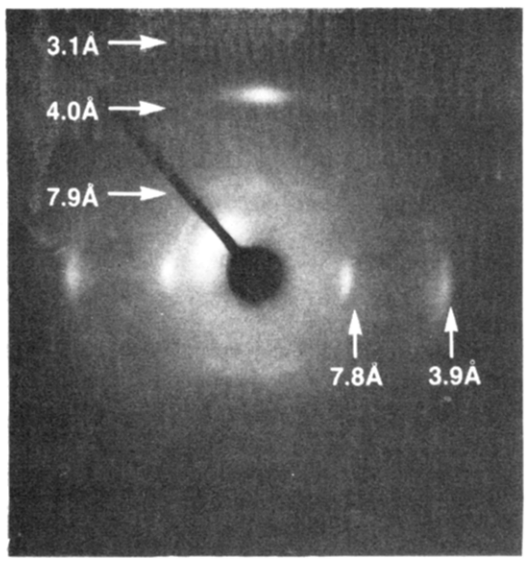


**Figure 6.** X-ray diffraction photograph of an oriented nylon 6 film showing only even orders of the equatorial 15.6-Å repeat along with meridional reflections at 7.9 (weak), 4.0, and 3.1 Å (diffuse).

not applied, and hence the peak was incorrectly reported as a 4.55-Å reflection. The asymmetry in these reflections suggests the presence of numerous faults corresponding to displacements of the iodide ion columns with vector component along the chain axis of nylon 6 (see "Structure of Iodide Ions in the Complex" under Discussion). The coherence length as calculated by using the Scherrer equation[9] is ~38 Å for the 4.75-Å peak and ~30 Å for the 3.2- and 3.08-Å peaks.

Small-angle X-ray scattering (SAXS) results show that although the lamellar peak is barely visible in oriented precursor samples (drawn 1:3 at room temperature), it is extremely intense (Bragg spacing = 98 Å) in freshly prepared iodine–nylon 6 complex (Figure 7A). The intensity of this SAXS peak rapidly decreases by a factor of 30 in the first 5 min of washing in aqueous sodium thiosulfate (Figure 7B). This is accompanied by a weakening of the 15.6-Å equatorial series and the appearance of the 8-Å meridional peak; the meridional reflections at 4.75, 4, 3.1 Å remain essentially unchanged (Figure 7B, wide-angle XRD photograph). Further washing for 27 min and an 8-h exposure to air result in a gradual decrease in SAXS intensity to zero (Figure 7C). This is accompanied by the disappearance of the 15.6-Å equatorial series and the 4.75-Å meridonal peak, weakening of the 3.1-Å meridional

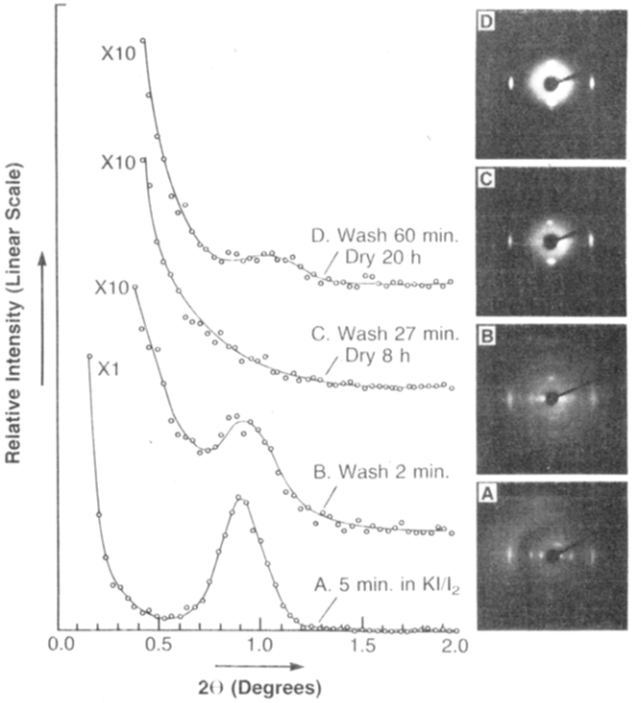


**Figure 7.** Small-angle X-ray scattering curves of uniaxially oriented iodinated nylon 6 film at various stages of iodine desorption. Each SAXS curve is accompanied by a wide-angle XRD photograph of an equivalent sample (A) or of samples immediately after the SAXS experiment (B, C, and D). Note the change in the vertical scale for curve A.

streak, and a gradual increase in the intensity of the 8-Å meridional reflection of nylon 6 chains (Figure 7C, photograph). Upon washing for 1 h and a 12-h exposure to air, the SAXS peak reappears with an intensity (Bragg spacing = 83 Å) expected for highly crystalline oriented nylon 6 (Figure 7D), and the wide-angle XRD pattern is typical of the $\gamma$ form of nylon 6 (Figure 7D, photograph). Note that the small-angle Bragg spacing, indicative of the separation of the lamallae, decreased from 98 Å in the complex to 83 Å in the $\gamma$ form. By cycling a fiber four times between the complexed and the desorbed states, we found that this spacing changes reversibly from 89 ± 3 Å in the iodine-free sample to 102 ± 4 Å in the iodinated sample. This might represent a reversible increase in the thickness of the amorphous layer in the presence of $KI/I_2$, or it might reflect a reversible change in the shape of the electron-density profile across the lamallae, i.e., along the chain axis.

## Discussion

**Diffusion of Iodide Ions.** It is generally known that many dye, water, and gas molecules diffuse preferentially into the amorphous regions in semicrystalline polymers. If iodine diffused only into the amorphouse regions, resulting in a crystalline complex with the amorphous component, then crystalline nylon 6 reflections should be observable in the complex. This is contrary to our experimental findings. In particular, when we start with the $\gamma$ form of nylon 6, the intense meridional (020) reflection is not seen in the complex. The same crystalline complex is obtained irrespective of whether the starting film is in the $\alpha$ or the $\gamma$ crystalline form or is completely amorphous. Thus iodine diffuses into both amorphous and crystalline forms and yields a crystalline complex with a 15.6-Å repeat and a 4.3-Å reflection in the equatorial plane and 4.75, 3.2-, and 3.08-Å reflections along the fiber axis.

Elemental analyses of nylon–iodine complexes show significantly a higher mole fraction of iodine than potas-

sium: $NI_{0.8}K_{0.2}$ in freshly prepared films and $NI_{0.3}K_{0.002}$ in films washed for 5 min in a 0.1 M aqueous solution of $Na_2S_2O_3$. In general, such elemental analyses, as well as X-ray fluorescence analysis, showed very little potassium in partially washed films and in films aged for several days under ambient conditions. Since $NI_{0.8}K_{0.2}$ can be written by expressions such as $N[(I_5^- K^+)_{0.5}(I_3^- K^+)_{0.5}]_{0.2}$, there are probably sufficient potassium ions ($K^+$) in fresh films to balance the negative charge of the iodide ions. It appears that iodide ions leach out of the film at a much slower rate than potassium ions, and in partially desorbed films the negative charge of the iodide ion is probably balanced by $H^+$. A more detailed analysis on a second set of fresh films ($N(H_2O)_{0.2}H_{1.1}I_{0.75}K_{0.15}Na_{0.01}S_{0.003}$; total weight percent of these elements is 99.93%) and on 5-min-washed films ($N(H_2O)_{0.3}H_{1.4}I_{0.24}K_{0.0004}Na_{0.03}S_{0.05}$; total weight percent of these elements is 100.00%) supports this conclusion.

The intense small-angle peak (Figure 7A) suggests that the distribution of the ions ($K^+$, $I_3^-$, and $I_5^-$) is modulated by the lamellar structure of nylon 6. Let us consider if the large small-angle intensity is due to the higher concentration of ions in the amorphous region, as observed with dye molecules. The most lightly iodine complexed crystal lattice (Figure 9D; see "Structure of Nylon 6–Iodine Complex") gives a stoichiometry of $NI_{0.8}$ for the crystalline regions. Since SAXS intensity in iodinated nylon 6 is more than 30 times that of the desorbed nylon 6 (Figure 7A,D), the electron density should be ~6 times higher in the amorphus regions. With a typical crystallinity of 50%, the stoichiometry for the entire sample would be ($NI_{0.8}$ + $NI_{4.8}$), i.e., $NI_{2.8}$, which is far from the measured value of $NI_{0.8}$. Let us now consider the other alternative in which the large SAXS intensity in iodinated nylon 6 is due to a higher concentration of the ions in the crystalline regions. The stoichiometry for the crystalline lattice of the complex shown in parts A and B of Figure 9 would be $NI_{2.1}$ and $NI_{1.2}$, respectively. If we now assume 6 times fewer ions in the amporhous regions, the stoichiometry for the entire sample would be $NI_{1.2}$ or $NI_{0.7}$, which is closer to the measured value of $NI_{0.8}$. It is unlikely that the inclusion of the potassium ions in the above argument will change the final conclusion that the concentration of the ions is higher in the crystalline regions than in the interlamellar amorphous regions. This nonuniform distribution of potassium and iodide ions might in part result from different rates of desorption of these ions from crystalline and amorphous regions.

On the basis of previous Raman[10] and X-ray[7] data, it was concluded that $I_3^-$ species are desorbed during the earlier stages of desorption. Wet chemical analysis shows a 100 times decrease in potassium while iodine decreases only by a factor of 3. Therefore, it appears that the nearly 30-fold decrease in SAXS intensity is accompanied by a loss of most of the $K^+$ and $I_3^-$ ions. We speculate that $K^+$ and $I_3^-$ are bound together, thus balancing the charges on each other, and the disappearance of both these ions from the crystalline regions during the initial stages of desorption contributes to the loss of SAXS intensity (Figure 7A,B). It is likely that the charge on the $I_5^-$ (at least in the later stages of iodine desorption (I–I distance of 3.08 Å)) is balanced by the charge on the amide NH group, and this ion is lost more gradually from both crystalline and amorphous regions during the later stages of iodine desorption. These mechanisms might account for the loss of electron-density contrast (and hence SAXS intensity) at some point during iodine desorption (Figure 7C). Upon complete iodine desorption (there is some iodine detectable by X-ray fluorescence even in a thoroughly washed nylon 6 specimen), the contrast due to crystalline lamallae and the interlamellar amorphous regions might give rise to a small SAXS peak typical of orient semicrystalline nylon 6 (Figure 7D).

The increase in the crystallinity of the film, due to the formation of this iodine–nylon 6 complex, reduces further diffusion of iodide ions into the film. The might explain the observation that when a 1-mm-thick nylon 6 plaque is immersed in a I/KI solution the diffusion is limited to a distance of ~200 $\mu$m from the surface. During this recrystallization, the polymer chains in the unoriented amorphous regions immediately orient themselves along the direction of diffusion of iodide ions, which is normal to the plane of the film. We propose that this orientation is due to the specific interactions between the $I_5^-$ columns and the nylon 6 chains (see below). If the film is unoriented to begin with, then the oriented crystallization of the complex in the amorphous regions caused by the unidirectional diffusion of the iodide ions preferentially orients the polymer chains in the entire sample normal to the plane of the film. This orientation occurs immediately after the diffusion of iodide ions in nylon 6 films.

The polymer chains can be oriented normal to the surface of the film during iodination only in unoriented films. In preoriented films, uniaxial (drawn) or planar (rolled), the polymer chains or crystallites retain their initial orientation and do not reorient along the direction of diffusion of iodide ions. We have already attributed the orientation during $KI/I_2$ treatment of unoriented films to the oriented crystallization of the amorphous regions. In oriented films we propose that the amorphous regions are oriented in the precursor films and this orientation persists in the crystallized complex, and therefore the recrystallization is not accompanied by diffusion-induced orientation.

**Structure of Nylon 6–Iodine Complex.** Although the 4.3-Å reflection on the equator and the 4-Å (040) reflection on the meridian in the complex are due to a lattice defined by nylon 6 chains, they do not represent either the $\alpha$ or the $\gamma$ form. The 4.3-Å reflection represents the distance ($4.3/\sin\beta$, $\beta = 67°$) between H-bonded nylon 6 chains in (001) planes of the $\alpha$ form or ($h$00) planes of the $\gamma$ form of nylon 6. This suggests that the integrity of the H-bonded sheet (not necessarily the hydrogen bonds) is maintained in the presence of the iodide ions. This is further confirmed dramatically in Figure 2, which is a parafocus scan of an iodinated planar oriented nylon 6 film (hydrogen-bonded sheets parallel to the surface of the film). While the (200) reflection ($a$ axis along the hydrogen bonds) is not present in the parafocus scan, it is visible in the transmission photographs (not shown). Up to 12 orders of the 15.6-Å repeat in a direction perpendicular to the plane of the film suggest a layered arrangement of the iodide ions in which the distance normal to the crystallographically equivalent iodide ion sheets is 15.6 Å. Since H-bonded sheets in these precursor planar-oriented films are parallel to the plane of the films, it is possible that, at least in freshly prepared films in which the 15.6-Å series is visible, iodide ion sheets are intercalated between sheets of nylon 6 chains that were hydrogen-bonded prior to iodination.

The above results are in agreement with the infrared results of Arimoto,[11] who found that the transition moments ascribed to the methylene groups remain unchanged while those characteristic of the amide group are preferentially twisted roughly perpendicular to the rolled plane, which is also the plane of the hydrogen-bonded sheet before iodination. The integrity of the chains in the hy-

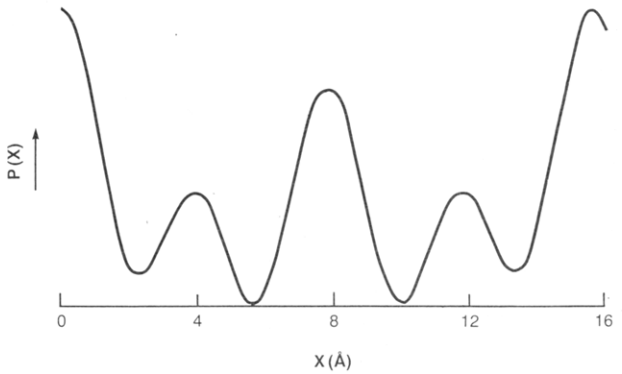


**Figure 8.** Patterson map of the equatorial reflections with 15.6-Å repeat period.

drogen-bonded sheets in the presence of iodine in nylon 6 is in contrast to the effect of iodine in polypeptides such as collagen where iodine breaks up the hydrogen bonds, leading to the collapse of the structure (unpublished results).

As an interesting aside, we analyzed the increases in the widths $\beta$ of the 10 orders of the 15.6-Å repeat as a function of the Bragg order $h$. Since the diffraction data were obtained in the parafocus mode, the profiles were closer to a Lorentzian. Therefore, one could plot $\beta$ vs. $h^2$ or $\beta$ vs. $h^4$ and verify respectively whether Hosemann's model of paracrystalline lattice or Warren's model of microstrain is appropriate for the layered structure of iodine–nylon 6 complex (see ref 12 for details of analyses). Preliminary analyses on three different planar-oriented iodinated films show that the full width of half-maximum $\beta$ obeys the relation $\beta = ah^2 + b$ instead of $\beta^2 = a'h^4 + b'$, $a$, $b$, $a'$, and $b'$ being constants, suggesting that the intercalated structure of iodine–nylon 6 probably forms a paracrystalline lattice.

A Patterson function was obtained from the equatorial reflections to determine the distribution of the iodide ion columns and nylon 6 chains in the complex. The intensities were corrected for Lorentz, polarization, and absorption factors. The Patterson curve in Figure 8 shows that the 4-Å peak is weaker than the 8-Å peak. The 4-Å peak might arise from iodine–nylon 6 interference and the 8-Å peak from iodine–iodine interference. Four possible models to explain the complexation of iodide ions into the nylon 6 lattice are schematically shown in Figure 9. In the first model (Figure 9A) all nylon 6 chains are hydrogen bonded to each other. In one iodine layer we have $I_5^-$ columns along the chain axis, and in the next iodine layer we have $I_3^-$ columns perpendicular to the chain axis. This model is in agreement with the interpretation of Raman spectroscopy data.[10] The differences in the electron density on either side of the nylon 6 sheet, possibly due to the differences in the packing of $I_5^-$ columns and $I_3^-$ arrays, might give rise to the 15.6-Å peak (Figures 1, 2A, and 4A), which is twice the width of one nylon 6 and one iodine sheet. In the second model (Figure 9B) the $I_3^-$ columns form a sheet, whereas the $I_5^-$ columns are surrounded by nylon 6 chains. In this second model, the electron density in the $I_3^-$ sheet is roughly 3 times that in the $I_5^-$ sheet. This can also explain the 15.6-Å repeat observed in the X-ray diffraction pattern. The third and the fourth models (parts C and D of Figures 9) are devised to explain the appearance of only even orders of the 15.6-Å repeat, i.e., a spacing of 7.8 Å in aged specimens (Figure 6). Although both the models have only $I_5^-$ species, Figure 9D might represent the complex during the final stages of iodine desorption.

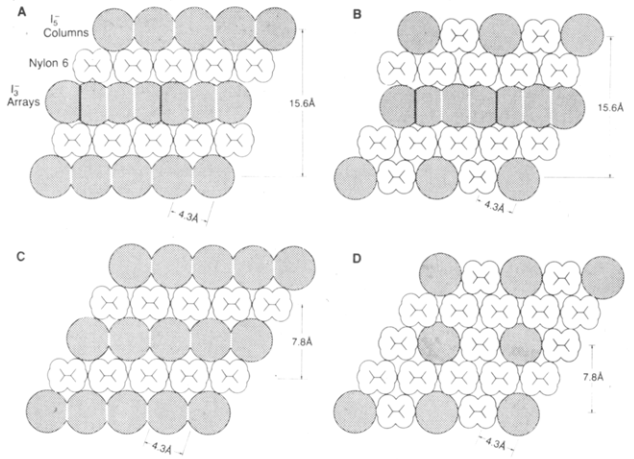


**Figure 9.** Models for the nylon 6–iodine complex showing iodide ion sheets (A, B, and C) and the iodide ion columns ($I_5^-$) in nylon 6 (B and D). Solid black lines in A and B delineate $I_3^-$ arrays (I–I distance is 3.1 Å, and $I_3^-$ repeat is 9.5 Å).

Notice that the models in parts B and D of Figure 9 require complete recrystallization, unlike the intercalation of iodide ions between sheets of nylon 6 chains in the models in parts A and C. It is probable that development of the $\gamma$ form may indeed require such recrystallization. Data we presently have are not sufficient to either further substantiate these claims or distinguish among these models.

There have been different interpretations of the infrared spectroscopy data on the question of coordination of the molecular iodine to the amide group. Arimoto[11] postulated that iodine coordinates with the oxygen atom. Abu-Isa,[13] on the basis of the premise that the oxygen of the carbonyl group is more basic than the nitrogen of the amide group, supported Arimoto's suggestion. But the model structures (substituted *N*,*N*-dimethylamides[14,15]) used by Abu-Isa are not appropriate for nylon 6. In contrast to this interpretation, Doskočilová and Schneider[16] concluded that the triiodide ion is coordinated with two NH groups. In support of this finding, Matsubara and Magill[17] presented IR data showing that the carbonyl group is either linked to $K^+$ cation or is protonated by $H^+$. Toman, Honzl, and Ječný[18] carried out X-ray crystallographic analysis of a polyiodide complex with *N*-methylacetamide and concluded that NH groups are linked to $I^-$ ions and CO groups to $K^+$ cations. Herbstein and Kapon[19] came to a similar conclusion from their crystal structure analysis of (phenactin)$_2$ $HI_5$. If we assume that the amide group in nylon 6 is similar to that in *N*-methylacetamide and phenactin, we have strong evidence to suggest that iodide ions (particularly $I_5^-$) coordinate with the NH and the CO of the amide group interacts with $K^+$ and $H^+$ in freshly prepared samples and with $H^+$ in aged specimens (ref 7 and 10; also see below).

**Structure of Iodide Ions in the Complex.** In the previous section we discussed how XRD data can be interpreted by a model in which two-dimensional sheets of iodide ions are intercalated between sheets of nylon 6 chains (Figure 9A,B,C). Resonance Raman spectroscopy[10] indicated $I_3^-$-like features normal to the chain axis and $I_5^-$ columns along the chain axis; upon desorption of iodine the $I_3^-$ features disappeared first. The XRD patterns (Figures 3 and 4) show that the decrease in the intensities of the equatorial 15.6-Å and meridional 4.75-Å reflections along with that of the 3.2-Å meridional band is followed by the disappearance of the meridional 3.08-Å band. On the basis of this XRD and Raman data, we conclude that both 3.2 and 3.08 Å correspond to the average iodine–

iodine distance in $I_5^-$ columns. The $I_5^-$ columns in our model (Figure 9) are parallel to the chain axis. The NH and the carbonyl groups in the nylon 6 chains adjacent to the $I_5^-$ columns are probably forced out of the $CH_2$ plane, and the resulting pleated sheet might interact favorably with $I_5^-$ columns. This might preclude similar interaction on the other side of the nylon 6 sheet. We speculate that iodide ions in this side of the sheet have $I_3^-$ features perpendicular to the chain axis of nylon 6 (Figure 9A) and are loosely bound. The 4.75-Å peak is present along the fiber axis in freshly complexed films in which $I_3^-$ ions are present (Raman spectra). This is greater than the van der Waals diameter of iodine of 4.3 Å and is, in fact, closer to the 4.64-Å separation of $I_3^-$ and $I^-$ ions.[18] We therefore speculate that the 4.75-Å meridional reflection might represent the separation of the nonbonded $I_3^-$ arrays.

As pointed out earlier (see Results), both 4.75- and 3.08-Å reflections and possibly the 3.2-Å reflection are asymmetric; they rise sharply on the low-angle side and have a longer tail on the high-angle side. Such asymmetric peaks have been discussed by Warner[20] and Wilson[21] with reference to layered structures such as clays and carbon. Jones[22] has shown how such asymmetric profiles can arise from one- and two-dimensional structures. The asymmetry of the 3.08- and 3.2-Å reflections in our case implies that iodide ion chains in adjacent channels are randomly displaced with respect to one another along the chain axis, with little correlation between the columns. The asymmetry of the 4.75-Å peak, if this is due to $I_3^-$ sheets, implies that, as in the case of clays and carbons, adjacent $I_3^-$ sheets are randomly displaced in the plane of the sheet, with little or no register between the neighboring sheets.

Diffractometer scans given in Figure 5 show the presence of two I–I distances, 3.2 and 3.08 Å. The 3.2-Å spacing is present only in freshly prepared films, and the 3.08-Å peak is seen even in the final stages of iodine disorption (Figure 3C). Since Raman data[10] suggest that both of these spacings are due to $I_5^-$ columns, we postulate the existence of two types of $I_5^-$ ions in the iodine–nylon 6 complex: in one the average I–I distance is 3.2 Å and in the the other this distance in the $I_5^-$ column is 3.08 Å. In the less stable form, the average iodine–iodine distance is longer (3.2 Å), probably because it interacts with the nylon 6 chains (which have a chain-axis repeat of $\approx$ 16.8 Å in the uncomplexed form and $\approx$ 16 Å in the complex) and forms a commensurate structure with the nylon 6 lattice (see below). Also, as the $I_3^-$ arrays disappear (Raman data;[10] 15.6-Å equatorial repeat changes to 7.8 Å and the intensity of the 4.75-Å meridional reflection decreases), the I–I distance in the $I_5^-$ column decreases from 3.2 to 3.08 Å. This suggests that only in the presence of $I_3^-$ arrays (Figure 9A,B) in the adjacent iodine sheet does the I–I distance in the $I_5^-$ column have a larger value of 3.2 Å. Both these factors, the commensurate structure with the nylon 6 chains and the presence of $I_3^-$ arrays, probably contribute to the stability of the otherwise unstable $I_5^-$ column with 3.2-Å I–I distance. On the other hand, the more stable form of $I_5^-$ with a shorter average iodine–iodine distance (3.08 Å) might not form a commensurate structure with nylon 6. The amide groups in aged and partially desorbed films are probably involved in hydrogen bonding between nylon 6, and this interchain H bonding increases the nylon 6 chain repeat to $\approx$ 16.8 Å, which is too long for an $I_5^-$ column. As the specimens are aged and the I/KI concentration decreases, it is likely that the $I_3^-$ feature of the iodide ion arrays in every other sheet gradually changes to yield $I_5^-$ columns. This complex, in which all iodide ions exist in the stable form of $I_5^-$ with an I–I distance of 3.08 Å (Figure 9C,D), persists until the final stages of iodine desorption.

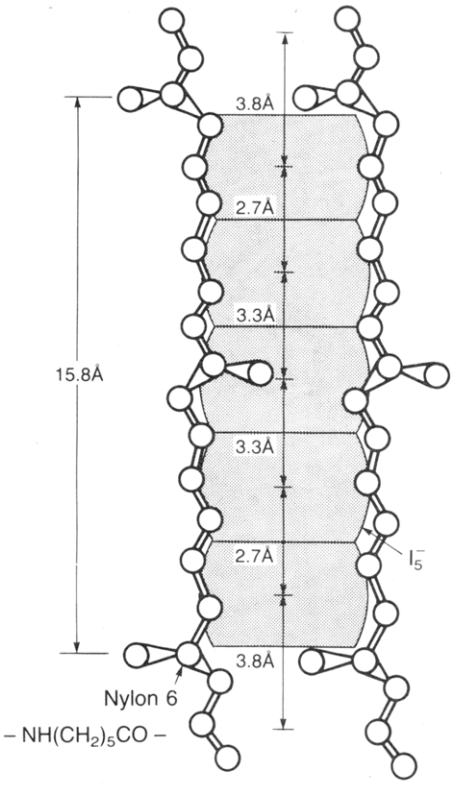


**Figure 10.** Proposed lattice match between $I_5^-$ columns and nylon 6 chains along the fiber axis.

**Lattice Match between Iodine-Ion Columns and Nylon 6.** On the basis of Raman spectroscopic evidence, we have already attributed both 3.2- and 3.08-Å meridional bands to $I_5^-$ columns in different states of order. We have also seen that the chain repeat of nylon 6 in freshly prepared iodine–nylon 6 complex is between 15.8 and 16.0 Å. Since an average I–I distance of 3.2 Å is observed in freshly prepared films, one can postulate that this $I_5^-$ unit spans two chemical or one crystallographic repeat of nylon 6. This can be accomplished by the arrangement shown schematically in Figure 10 by using the distances found by crystallographic analysis of iodine complexes of small organic molecules.[19,23,24] This model suggests that $I_5^-$ can be regarded as $I_2$–$I^-$–$I_2$ units. Such a model represents a highly ordered structure, and the disorder along the chain axis might be expected to yield the observed average iodine–iodine distance of 3.2 Å. This model shows specific attachments of either end of the $I_5^-$ ion to the amide nitrogen. According to this model adjacent $I_5^-$ columns need to be staggered by 8 Å (half the chain-axis repeat).

In addition to the lattice match between $I_5^-$ columns and nylon 6 chains along the fiber axis, it is also possible to postulate a match between nylon 6 chains and $I_5^-$ and $I_3^-$ arrays in the equatorial plane as well. The length of the $a$ axis of a nylon 6 unit cell, corresponding to the separation of the nylon 6 chains in the hydrogen bonded-sheet, is 9.5 Å. This is equal to the length of the $I_3^-$ arrays. Thus $I_3^-$ arrays could span two hydrogen-bonded chains. Also, note that the separation of the $I_5^-$ columns is the same as the distance between the hydrogen-bonded nylon 6 chains.

**Evolution of the γ Form.** In a freshly prepared complex, the chain repeat of nylon 6, as measured by the (040) reflection, is between 15.8 and 16.0 Å. The absence of the (020) reflection suggests that the amide groups in adjacent H-bonded sheets are staggered as in the $\alpha$ form of nylon

6. The shorter chain repeat of ≈16 Å (compared with the normal value of ≈16.8 Å for the γ form and 17.2 Å for the α form, and in fact the shortest reported for nylon 6), is probably due to the lattice match between the strained $I_5^-$ column (I–I distance of 3.2 Å) and the nylon 6 chains. This might represent a pleated arrangement of the hydrogen-bonded sheets. The shorter repeat of nylon 6 apparently initiates the formation of hydrogen bonds between parallel chains during iodine desorption, thus leading to the γ form. During the desorption of iodine, the loosely bound $I_3^-$ ions are first removed. This is accompanied by the decrease in the intensity of the 3.2-Å iodine–iodine interference peak, a gradual decrease in the intensity of the 15.6-Å series, and the onset of the meridonal (020) peak at 8 Å from the nylon 6 lattice. Upon further desorption of iodine, the 8-Å peak becomes more intense and shifts from 7.95 to 8.43 Å (chain repeat increasing from 15.9 to 16.9 Å). This sequence of changes suggests that as the $I_3^-$ ions are removed the interaction between $I_5^-$ and nylon 6 chains becomes weaker and the I–I distance in the $I_5^-$ columns springs back to the normal value of 3.1 Å from the strained 3.2-Å separation, while the nylon 6 repeat increases toward the normal value of 16.7–16.9 Å. During this iodine desorption, the amide groups in adjacent H-bonded sheets, which are probably staggered in the complex, are brought into alignment (increase in the intensity of the (020) reflection), thus yielding the γ form with H bonds between parallel chains and the amide groups of adjacent H-bonded sheets in one equatorial plane.

## Conclusion

$I_5^-$ and $I_3^-$ species of iodide ions are present in freshly iodinated nylon 6 as sheets intercalated between sheets of nylon 6 chains. The distribution of the $K^+$, $I_3^-$, and $I_5^-$ ions in an aqueous $KI/I_2$-treated nylon 6 film is modulated by the lamellar structure of nylon 6. $K^+I_3^-$ probably exists in the lamellar crystalline regions and is easily desorbed. $I_5^-$ columns exist in two forms: a less stable form with an I–I distance of 3.2 Å and a more stable form with an I–I distance of 3.08 Å. The lattice match between $I_5^-$ columns and nylon 6 chains reduces the chain-axis repeat, twists the amide groups out of the $CH_2$ plane, and forms hydrogen bonds between parallel chains. This leads to the formation of the γ form upon the removal of iodine.

**Acknowledgment.** I thank Prof. S. Krimm, Dr. J. P. Sibilia, and Mrs. A. C. Reimschuessel for extensive discussions and Dr. A. J. Signorelli and Prof. P. Coppens for reviewing the manuscript.

**Registry No.** KI, 7681-11-0; $I_3^-$, 14900-04-0; $I_5^-$, 22318-17-8; nylon 6–iodine complex, 66572-60-9.

## References and Notes

(1) Schneider, A. A.; Harney, D. E.; Harney, M. J. *J. Power Sources* **1980**, *5*, 15.
(2) Yamamoto, T.; Kurada, S. I. *J. Electroanal. Chem.* **1983**, *158*, 1.
(3) Shirakawa, H.; Louis, E. J.; MacDiarmid, A. G.; Chiang, C. K.; Heeger, A. J. *J. Chem. Soc., Chem. Commun.* **1977**, 578.
(4) Kinoshita, Y. *Makromol. Chem.* **1959**, *33*, 1.
(5) Holmes, D. R.; Bunn, C. W.; Smith, D. J. *J. Polym. Sci.* **1955**, *17*, 159.
(6) Haberkorn, H.; Simak, D.; Illers, K. H. *Eur. Polym. J.* **1975**, *11*, 547.
(7) Murthy, N. S.; Szollosi, A. B.; Sibilia, J. P.; Krimm, S. *J. Polym. Sci., Polym. Phys. Ed.* **1985**, *23*, 2369
(8) Murthy, N. S. *Norelco Rep.* **1983**, *30*(3), 35.
(9) Guinier, A. *X-ray Diffraction*; Freeman: San Francisco, 1963; pp 225–226.
(10) Burzynski, R.; Prasad, P. N.; Murthy, N. S. *J. Polym. Sci., Polym. Phys. Ed.* **1986**, *24*, 133.
(11) Arimoto, H. *J. Polym. Sci., Part A* **1964**, *2*, 2283.
(12) Murthy, N. S. *J. Polym. Sci., Polym. Phys. Ed.* **1986**, *24*, 549.
(13) Abu-Isa, I. *J. Polym. Sci., Polym. Chem. Ed.* **1971**, *9*, 199.
(14) Drago, R. S.; Wenz, D. A.; Carlson, R. L. *J. Am. Chem. Soc.* **1962**, *84*, 1106.
(15) Tsubomura, H.; Lang, R. P. *J. Am. Chem. Soc.* **1961**, *83*, 2085.
(16) Doskočilová, D.; Schneider, B. *Collect. Czech. Chem. Commun.* **1962**, *27*, 2605.
(17) Matsubara, I.; Magill, J. H. *Polymer* **1966**, *7*, 199.
(18) Toman, K.; Honzl, J.; Ječný, J. *Acta Crystallogr.* **1965**, *18*, 673.
(19) Herbstein, F. H.; Kapon, M. *Philos. Trans. R. Soc. London* **1979**, *291*.
(20) Warren, B. E. *Phys. Rev.* **1941**, *59*, 693.
(21) Wilson, A. J. C. *Acta Crystallogr.* **1949**, *2*, 245.
(22) Jones, R. C. *Acta Crystallogr.* **1949**, *2*, 252.
(23) Endres, H.; Keller, H. J.; Megnamisi-Belombe, M.; Morani, W.; Pritzkow, H.; Weiss, J. *Acta Crystallogr., Sect. A: Cryst. Phys., Diffr., Theor. Gen Crystallogr.* **1976**, *A32*, 954.
(24) Herbstein, F. H.; Kapon, M. *Acta Crystallogr., Sect. A: Cryst. Phys., Diffr., Theor. Gen. Crystallogr.* **1972**, *A28*, 574.